

## N-doped anodic titania nanotube arrays for hydrogen production

Sang-Sun Park\*, Seon-Mi Eom\*\*, Masakazu Anpo\*\*\*, Dong-Ho Seo\*, Yukwon Jeon\*, and Yong-gun Shul\*<sup>\*,\*\*†</sup>

\*Department of Chemical Engineering, Yonsei University, 134 Shinchon-dong, Seodaemun-gu, Seoul 120-749, Korea

\*\*The Specialized Graduate School of Hydrogen & Fuel Cell, Yonsei University,  
134 Shinchon-dong, Seodaemun-gu, Seoul 120-749, Korea

\*\*\*Department of Applied Chemistry, Graduate School of Engineering, Osaka Prefecture University,  
1-1 Gakuen-cho, Naka-ku, Sakai, Osaka 599-8531, Japan

(Received 4 October 2010 • accepted 1 December 2010)

**Abstract**—Titanium dioxide ( $TiO_2$ ) nanotube arrays are grown in a mixed electrolyte by anodizing process. The anodic nanotubes for N-doping were calcinated at 773 K in a tube furnace with a mixture of  $NH_3$  and Ar gas. The photocatalytic activity of N-doped  $TiO_2$  nanotubes was carried out in a water-splitting reaction under UV and visible light irradiation. Various characterization techniques (Scanning electron microscopy, X-ray diffractometry, X-ray photo-electron spectroscopy, etc.) are used to study the surface morphology, phase of structure, and binding energy.

Key words: Anodization, Hydrogen,  $TiO_2$  Nanotube, Water-splitting

## INTRODUCTION

Photocatalysts to generate hydrogen through water splitting in solar energy contribute to environmentally friendly programs due to their properties as a clean source and zero emission. Among them,  $TiO_2$  is a promising candidate because of its relatively low cost, non-toxicity, stability, and high yield. So,  $TiO_2$  photocatalysts have attractive advantages for various industrial fields such as the purification of toxic compounds in polluted water and air [1,2]. And, these substances have been employed as materials for water splitting and in solar cells, recently [4-9].

Among several types of  $TiO_2$  photocatalysts,  $TiO_2$  nanotubes may be of great use for photovoltaics, photocatalysis, photoelectrolysis, and photo sensors, due to their unique properties originating from their unique nanotubular structure [2,3,6,7]. It was already known that  $TiO_2$  nanotubes had more optimal properties in comparison to other  $TiO_2$  compounds with nanocrystalline structures. Several techniques including hydrothermal treatment, templating depositions and electro spinning have been mainly used to prepare  $TiO_2$  nanotubes [3-7]. Recently, the anodization process has been focused on by many researchers because its process is relatively simple to obtain ordered  $TiO_2$  nano-array with a large surface area [9,10]. In various preparation methods for  $TiO_2$  nanotubes, anodization of  $TiO_2$  in electrolytes, including fluorinate, is the simplest fabrication method to prepare tubular  $TiO_2$  [4].

However, a typical  $TiO_2$  catalyst can be activated only under UV light irradiation. To overcome these barriers, the development of vis- $TiO_2$  must be strongly required [3]. A few researchers have reported about visible response  $TiO_2$ , such as metal ion implanted  $TiO_2$  and anion doped  $TiO_2$  [3-5]. Simple preparation methods such as the RF magnetron sputtering deposition method were developed simultaneously [5]. The enlargement of surface area is significant and can

help to achieve a high activity of  $TiO_2$  under visible light irradiation as well.  $TiO_2$  nanotubes may be a well-qualified selection to fill in conditions that were explained previously [3-5]. Recently, many researchers have been working to develop  $TiO_2$  by anion doping, such as doping N, C, and S into the lattice [3-5,10,11]. The combined p states in the doped anion and O 2p states in the  $TiO_2$  shift the valance band edge upward to reduce the band gap energy of  $TiO_2$ . As a result, it is possible for  $TiO_2$  to have photo-electrochemical activity under visible light irradiation.

In the present work, we prepared  $TiO_2$  nanotube arrays using an anodization process with fluorinated electrolyte. Anodized nanotube arrays were hydrothermally treated at mixed gas atmosphere with  $NH_3$ /Ar in order to improve the photo electrochemical activity under visible light irradiation [3]. Prepared visible response  $TiO_2$  nanotube arrays were employed as an anodic substrate to generate hydrogen in the water splitting system.

## EXPERIMENTAL

### 1. Preparation of N-doped $TiO_2$ Nanotube Arrays

The titania nanotube arrays were fabricated by an anodizing process with Ti foil (0.1 mm thickness, 99.5% purity, Nilaco Japan) as anode and Pt gauze (100 mesh, 99.9% purity, Sigma-Aldrich, USA) as counter electrode [8]. Ti foil substrate was washed with acetone and ethanol, in turn, then was rinsed with DI water prior to use. Ti foil was anodized at voltage of 20 V in aqueous solution with 0.5 M  $H_3PO_4$ /0.1 M  $NaNO_3$ /0.14 M NaF for 6 h. The distance between Ti foil and Pt gauze is 2 cm. Then, anodic nanotubes were washed with DI water and dried in a furnace at 373 K for 24 h. N-doped  $TiO_2$  nanotube arrays were obtained from calcination in a tube furnace with mixed gas with  $NH_3$ /Ar at 773 K for 3 hours.  $NH_3$  flow rate was 50 ml/min and Ar flow rate was 350 ml/min.

### 2. Characterization

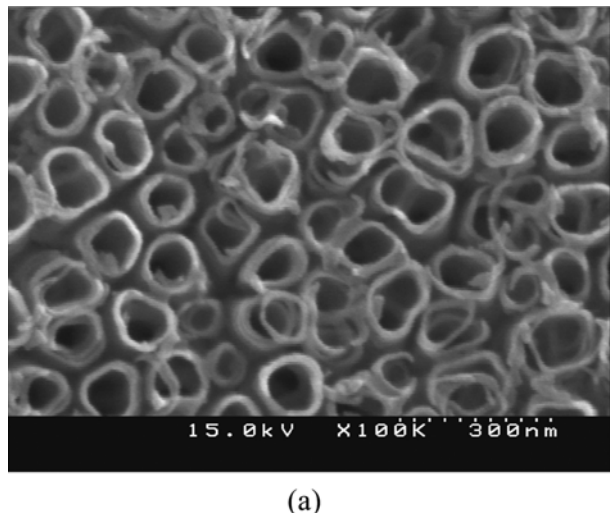
The  $TiO_2$  and N-doped  $TiO_2$  nanotubes were characterized by various measurements. The crystalline structure of the arrays was

\*To whom correspondence should be addressed.  
E-mail: shulyg@yonsei.ac.kr

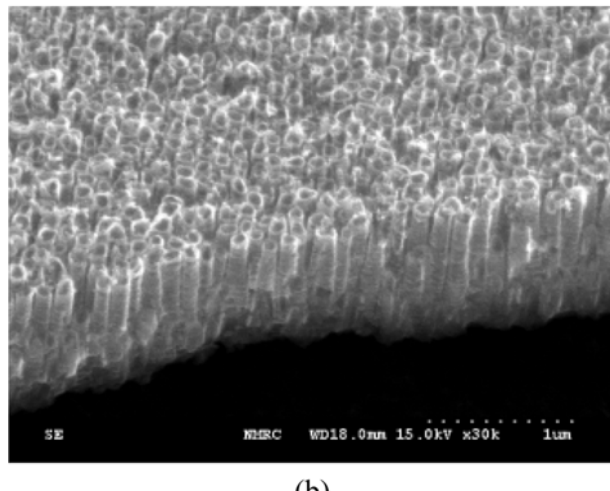
identified via X-ray diffraction analysis (XRD, Rigaku miniflex II, Japan) with Cu K $\alpha$  radiation source in the angle range of 20°–80°. The morphology and size of the arrays were investigated by a scanning electron microscope (SEM, HITACHI S-4300, Japan). The chemical binding energy of N-doped TiO<sub>2</sub> nanotubes was characterized with X-ray photoelectron spectroscopy (XPS, EscaLab 220-IXL system) with an aluminum filament by using the K $\alpha$  line. The optical absorption edge and band gap of the nanotubes were measured with a UV-Vis spectrophotometer (Optizen2120UV).

### 3. Hydrogen Generation

The photocatalytic experiment of N-doped TiO<sub>2</sub> nanotubes was carried out by water-splitting reaction under UV and visible light irradiation. A 300W Xe arc lamp was used as a light source. N-doped TiO<sub>2</sub> nanotube arrays were used as a photo-anode; the other side of the photo-anode was deposited with platinum particles using the RF-MS method and was used as a counter electrode. Prior to the water-splitting reaction, the inside of the reactor was purged of air with Ar (99.9% purity) gas for 3 hrs. Generated hydrogen was analyzed with a gas chromatograph (Young-Lin, Acme 6000 GC, Korea) with a thermal conductivity detector (TCD).



(a)



(b)

**Fig. 1.** SEM images of anodic TiO<sub>2</sub> nanotube arrays formed in 0.5 M H<sub>3</sub>PO<sub>4</sub>+0.1 M NaNO<sub>3</sub>+0.14 M NaF at 20 V for 6 h. (a) Top view, (b) cross-sectional view.

## RESULTS AND DISCUSSION

### 1. SEM

Fig. 1(a) and (b) show the cross-sectional and top view images of TiO<sub>2</sub> nanotube arrays grown by anodizing process. These arrays were prepared upon anodization of Ti foil in 0.5 M H<sub>3</sub>PO<sub>4</sub>+0.1 M NaNO<sub>3</sub>+0.14 M NaF aqueous electrolyte at 20 V for 6 hrs. Well-ordered TiO<sub>2</sub> nanotube arrays with narrow pore size distribution were obtained using these conditions. Anodized TiO<sub>2</sub> nanotubes have length in the range between 800 nm and 1.0 micron and their average pore diameter was about 20 nm.

### 2. X-ray Diffraction (XRD) Pattern

The crystal structure of the anodic TiO<sub>2</sub> nanotubes was characterized with an X-ray diffractometer. Fig. 2 shows XRD patterns of the resultant N-doped TiO<sub>2</sub> nanotubes after annealing in NH<sub>3</sub>/Ar mixed gas at 500 °C for 3 h and the non-treated TiO<sub>2</sub> nanotubes after annealing in air at the same condition and pure Ti-foil as reference. From XRD data, as shown in Fig. 2(b) and 2(c), all the anodic TiO<sub>2</sub> nanotubes had mixed phase with anatase and rutile suggesting that both samples had similar XRD patterns without any change of peak position. Thus, the intensity of rutile structure increased after annealing with NH<sub>3</sub>/Air mixed gas, indicating that the content of TiO<sub>2</sub> with

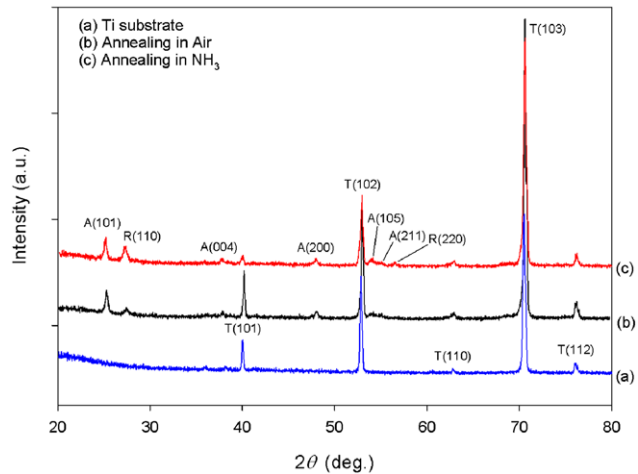
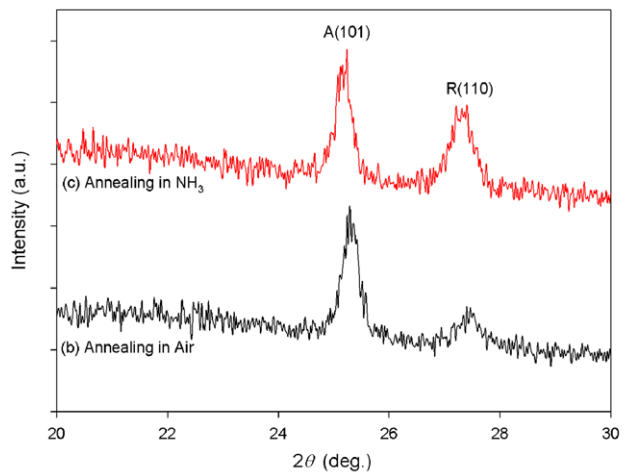


**Fig. 2.** X-ray diffraction patterns of (a) Ti foil surface, (b) anodic TiO<sub>2</sub> nanotubes annealed in air at 500 °C for 3 h and (c) sample annealed in Ar/NH<sub>3</sub> mixture gas at 500 °C for 3 hrs.

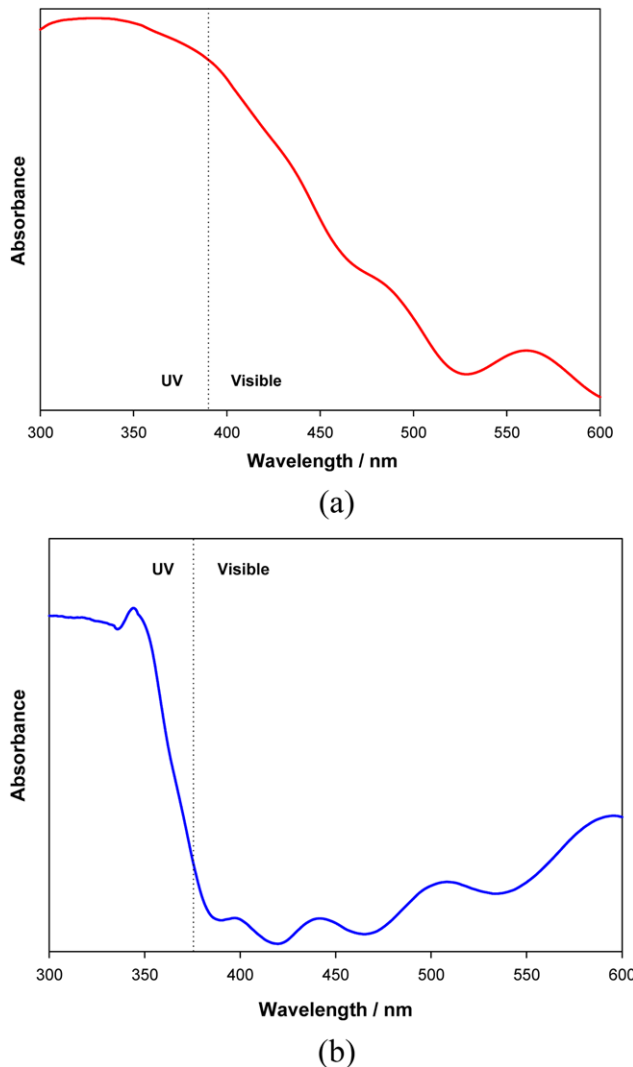


**Fig. 3. UV-Vis absorption spectra of the non N-doped  $\text{TiO}_2$  nanotube and N-doped  $\text{TiO}_2$  nanotube (b).**

rutile structure was enhanced by nitrogen ion implantation during the annealing step.

### 3. UV-VISIBLE

Fig. 3 shows the UV-Visible absorption spectra observed by  $\text{TiO}_2$  and N-doped  $\text{TiO}_2$  at different heat treatment conditions. After sample was calcinated in air, its absorption in the visible region was extremely decreased. On the other hand, the  $\text{TiO}_2$  nanotubes calcinated in  $\text{NH}_3$  showed wide absorption band in the range from 380 to 550 nm, suggesting that it has wide absorption over visible region [12]. For these anion-doped  $\text{TiO}_2$  photocatalysts, the mixing of the p states of the doped anion (N, S, C) with the O 2p states was reported to shift the valence band edge upwards to narrow the band gap energy of  $\text{TiO}_2$  [16]. So, the optical band edge of the N-doped  $\text{TiO}_2$  exhibits a remarkable red-shift compared with that of nontreated  $\text{TiO}_2$  [15]. Finally, the enhanced ability to absorb visible light makes N-doped  $\text{TiO}_2$  an effective photocatalyst for solar-driven applications [15].

### 4. X-ray Photoelectron Spectroscopy (XPS)

Fig. 4 shows the N1s X-ray photoelectron spectroscopy spectra of the N-doped  $\text{TiO}_2$  nanotubes prepared by hydrothermal process.

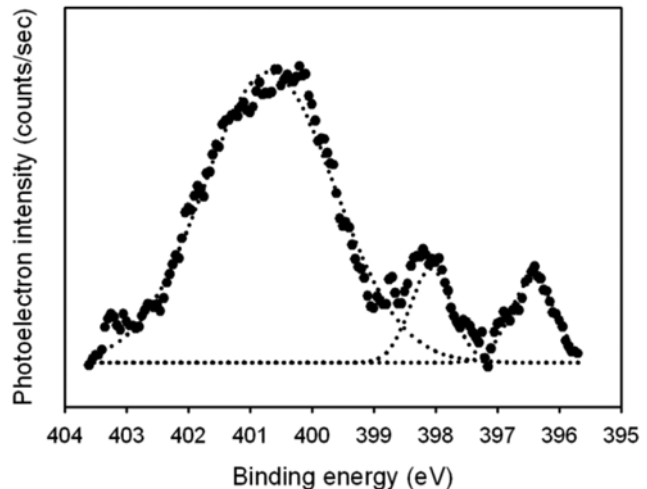


**Fig. 4. XPS data of the N-doped  $\text{TiO}_2$  nanotubes.**

In general, the peak of N1s from the XPS spectra was mostly found in the range of 396–404 eV [18]. In Fig. 4, nitrogen 1s core level peaks were observed at 400.7 eV, 398.1 eV and 396.4 eV. The peak at 396.4 eV was derived from Ti-N linkage when the N atom replaced the oxygen sites within the  $\text{TiO}_2$  lattice [17]. On the other hand, the N 1s peak at 398.2 eV was caused by the  $\text{N}^+$  anion species in the  $\text{TiO}_2$  as an N-Ti-O structural feature [13]. Many researchers have indicated that the presence of oxidized nitrogen (or oxidized Ti-N) such as Ti-O-N (or Ti-N-O) linkages should appear above 400.2 eV [13,19,20]. In this XPS result, the peak at a binding energy of 400.2 eV is ascribed to Ti-O-N or Ti-N-O bond in N-doped  $\text{TiO}_2$ . This linkage comes from the N atoms' substitution for titanium or both titanium and oxygen (NO, or  $\text{NO}_2$  type species appear above 400 eV) [13,14,21].

### 5. Water-splitting Reaction

Fig. 5 shows the time profiles of the hydrogen production during water-splitting reactions under UV (300–380 nm) and visible (420 nm+) light range. The water-splitting reactor consists of N-doped  $\text{TiO}_2$  nanotubes, Pt as counter electrode, and an ionically conductive separating membrane. The surface of the photo-anode with nanotubes was irradiated by light source of 300 W Xe arc lamp with glass filters. Hydrogen generation was detected in the presence of both UV and visible light irradiation. The amount of hydrogen generated from the  $\text{TiO}_2$  nanotube after UV light irradiation at reaction condition for 7 hours was about 270  $\mu\text{mol}$ . On the other hand, in case of the N-doped  $\text{TiO}_2$  nanotube, the production amount of hydrogen was 280  $\mu\text{mol}$ .

As shown in Fig. 5(a), in the visible region, the hydrogen production rate of N-doped  $\text{TiO}_2$  nanotubes increased with a good linearity in proportion to time. N-doped  $\text{TiO}_2$  nanotubes exhibited better activity than  $\text{TiO}_2$  nanotubes. The evolution rate of the hydrogen on N-doped  $\text{TiO}_2$  nanotubes was calculated at about 4.3  $\mu\text{mol}/\text{h}$ . However,  $\text{TiO}_2$  nanotube showed the relatively low activity compared to the N-doped  $\text{TiO}_2$  nanotube. Thus, N-doped  $\text{TiO}_2$  nanotubes were prior to the  $\text{TiO}_2$  nanotubes in generation of hydrogen. From these results, N-doped  $\text{TiO}_2$  nanotubes exhibited the better performance for water-splitting compared with  $\text{TiO}_2$  nanotubes annealed in air conditions.

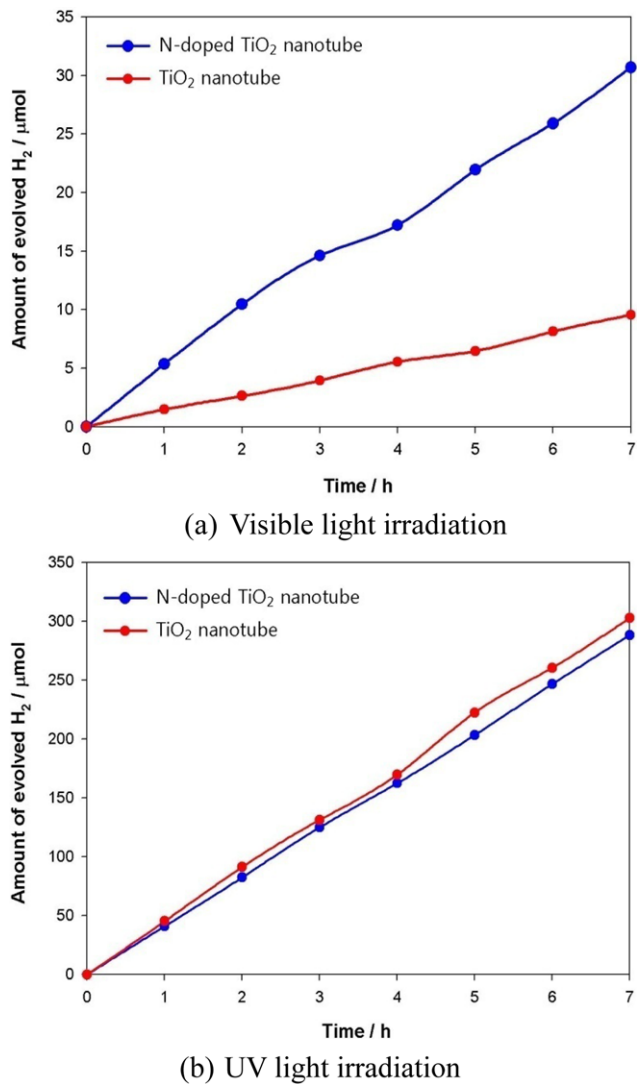


**Fig. 5. The amount of generated hydrogen from N-doped  $\text{TiO}_2$  nanotubes and non N-doped  $\text{TiO}_2$  nanotubes under the Xe lamp with cut-off filter. (a) Visible light irradiation (b) UV light irradiation A photo-anode area was  $4 \text{ cm}^2$  ( $10 \text{ mm} \times 40 \text{ mm}$ ).**

## CONCLUSIONS

Highly ordered  $\text{TiO}_2$  nanotube arrays by anodization of Ti foil were prepared in aqueous electrolyte. N-doping of  $\text{TiO}_2$  nanotube array was carried out by the hydrothermal deposition of elemental nitrogen with  $\text{NH}_3$ . From the SEM measurement and XRD data, it is confirmed that this is a good method to easily dope elemental nitrogen into the  $\text{TiO}_2$  lattice. XPS results reveal that N-doped  $\text{TiO}_2$  can exist as an N-Ti-O structure in the lattice. A high photo-catalytic activity for hydrogen generation by water-splitting in visible light irradiation has been observed for the N-doped  $\text{TiO}_2$  nanotubes. Moreover, the visible light-responsive  $\text{TiO}_2$  nanotube can be used as a

photo-anode in dye sensitized solar cells (DSSCs).

## ACKNOWLEDGEMENTS

This work was supported by the NEW & Renewable Energy R&D program (2009T100100606) under the Ministry of Knowledge Economy, Republic of Korea and this work was supported by the Human Resources Development of the Korea Institute of Energy Technology Evaluation and Planning (KETEP) grant funded by the Korea government Ministry of Knowledge Economy (No. 20104010100500).

## REFERENCES

- J. Zhao, X. Wang, T. Sun and L. Li, *J. Alloy Compd.*, **434-435**, 792 (2007).
- M. Paulose, Gopal K. Mor, Oomman K. Varghese, K. Shankar and Craig A. Grimes, *J. Photoch. Photobio. A*, **178**, 8 (2006).
- M. Matsuoka, M. Kitano, S. Fukumoto, K. Iyatani, M. Takeuchi and M. Anpo, *Catal. Today*, **132**, 159 (2008).
- S. Kaneko, Y. Chen, P. Westerhoff and John C. Crittenden, *Scripta Mater.*, **56**, 373 (2007).
- D.-J. Yang, H.-G Kim, S.-J. Cho and W.-Y. Choi, *Mater. Lett.*, **62**, 775 (2008).
- Y. Yang, X. Wang and L. Li, *Mater. Sci. Eng. B-Solid.*, **149**, 58 (2008).
- Kong C. Tep, Karthik Shankar and Craig A. Grimes, *NSF EE REU PENN STATE Annual Research Journal*, **3**, 142 (2005).
- K. S. Raja, M. Misra and K. Paramguru, *Electrochim. Acta*, **51**, 154 (2005).
- R. P. Vitiello, J. M. Macak, A. Ghicov, H. Tsuchiya, L. F. P. Dick and P. Schmuki, *Electrochim. Commun.*, **8**, 544 (2006).
- J. Jitputti, S. Pavasupree, Y. Suzuki and S. Yoshikawa, *J. Solid State Chem.*, **180**, 1743 (2007).
- A. Fujishima and K. Honda, *Nature*, **238**, 37 (1972).
- S. K. Mohapatra, M. Misra, V. K. Mahajan and K. S. Raja, *J. Catal.*, **246**, 362 (2007).
- M. Sathish, B. Viswanathan, R. P. Viswanath and S. Gopinath, *Chem. Mater.*, **17**, 6349 (2005).
- F. Peng, L. Cai, L. Huang and H. Yu, *J. Phys Chem Solids.*, **69**, 1657 (2008).
- J.-h. Xu, W. L. Dai, J. Li, Y. Cao, H. Li, H. He and K. Fang, *Catal. Commun.*, **9**, 146 (2008).
- M. Kitano, M. Matsuoka, M. Ueshima and M. Anpo, *Appl. Catal. A: Gen.*, **325**, 1 (2007).
- N. C. Saha and H. G. Tompkins, *J. Appl. Phys.*, **72**, 3072 (1992).
- Z. Wu, F. Dong, W. Zhao and S. Guo, *J. Hazard. Mater.*, **157**, 57 (2008).
- H. Sun, Y. Bai, Y. Cheng, W. Jin and N. Xu, *Ind. Eng. Chem. Res.*, **45**, 4971 (2006).
- E. Gyorgy, A. Perez del Pino, P. Serra, J. L. Morenza, *Surf. Coat. Technol.*, **173**, 265 (2003).
- X. Chen and C. Burda, *J. Phys. Chem. B*, **108**, 15446 (2004).